H. Ghanaati MD[1]
M. Motevalli MD[2]
A. Tabib MD[3]
A. Almasi MD[2]
F. Noohi MD[4]
M. Zabeti MD[5]

Multidetector CT Evaluation of Congenital Heart Disease: A Pictorial Essay

Multidetector computed tomography (MDCT) with or without ECG-synchronized images can successfully evaluate cardiac morphology and congenital heart diseases which mainly involve great vessels. In this pictorial essay, we present the great capability of MDCT for the evaluation of complex congenital heart disease.

Keywords: multidetector computed tomography, heart defects, congenital

Introduction

Echocardiography is the initial diagnostic modality for a patient with suspected congenital heart disease. In some patients, however, use of this modality is encumbered by its limited ability to delineate great arteries and intracardiac anomalies, pulmonary veins, and coronary arteries. Diagnostic cardiac catheterization, which has a small but well-known risk, is usually performed if echocardiography fails to provide a confident evaluation of the lesion. Despite its excellent anatomic and functional assessment capabilities, MR imaging is often limited in evaluation of seriously-ill or uncooperative patients; its use is contraindicated for patient with pacemaker.[1-3] MR imaging studies are time-consuming and may require patient sedation. Although the role of electron beam CT has been established in the evaluation of congenital heart disease, little has been reported on the evaluation of congenital heart disease using MDCT.[4,5] This article highlights the role of MDCT in the evaluation of congenital heart disease in certain problematic cases.

Technique

All MDCT evaluations were preceded by consulting with our pediatric and adult cardiology colleagues. Most of the studies were performed to answer specific anatomic questions raised by an inconclusive echocardiographic or angiographic evaluation. All studies were performed on an MDCT unit (Siemens, somatom sensation 10).

In pediatric groups who needed sedation we orally administered chloral hydrate (50-100 mg/kg) and if necessary, patient underwent a light intravenous sedation for 4–5 min by an anesthesiologist.

Nonionic contrast medium was administrated at a dose of 1–2 mL/kg with 240–320 mg/mL iodine concentration through a 20 or 22 G intravenous catheter in the patient's arm or leg with power dual injector at a rate of 1.5–4 mL/s and saline chaser. The bolus tracking marker was placed on the anatomic location of clinical question.

We used from low radiation dose technique according to the patient weight.

1. Associated Professor of Radiology, Medical Imaging Center, Imam Khomeini Hospital, Tehran University of Medical Sciences, Tehran, Iran.
2. Assistant Professor, Department of Radiology, Shahid Radjai Cardiovascular Medical Center, Iran University of Medical Sciences, Tehran, Iran.
3. Assistant Professor, Department of Pediatric Cardiology and Intensive Care Unit, Shahid Radjai Cardiovascular Medical Center, Iran University of Medical Sciences, Tehran, Iran.
4. Professor, Department of Cardiology, Shahid Radjai Cardiovascular Medical Center, Iran University of Medical Sciences, Tehran, Iran.
5. Anesthesiologist, Imam Khomeini Hospital, Tehran University of Medical Sciences, Tehran, Iran.

Corresponding author:
Marziyeh Motevalli
Address: Department of Radiology, Shahid Radjai Cardiovascular Medical Center, Vali-e-Asr St., Tehran, Iran.
Tel:+9821-23922415
Fax:+9821-22042026
Email: motavali_m@yahoo.com

Received December 21, 2006;
Accepted after revision March 1, 2007.

Iran. J. Radiol. Summer 2007;4(4):209-16

Twenty to 30 mAs were used for those under three years old; 40–100 mAs for those weighted 25–55 kg; 100–140 mAs for patients weighted >55 kg; 60 kV for patients weighted <45 kg; and 100–120 kV for those weighted ≥45 kg.The slice thickness was 1–2.5 mm with 50% reconstruction overlap and a pitch of one. The acquired axial slices reconstructed in sagittal and coronal planes. Furthermore, multiplanar reformatted images (MPR), maximum intensity projection (MIP) and volume rendering technique (VRT) were used.

Scans began from the root of neck for evaluation of supra-aortic arch branches to below the diaphragm. If total aorta or venous system or abdominal structures were target organs, examination was extended to the level of iliac crest. The time for scan was 5–12 s. Radiologist had access to unlimited numbers of reconstructed images in two workstations (volume navigator and volume wizard), reviewed images and could rotate images to observe the target organ from any view.

The images consisted of all anatomic structures of thorax including aorta and its branches, pulmonary artery and its branches, pulmonary veins and types of their returns, superior vena cava (SVC), inferior vena cava (IVC) and other veins, cardiac chambers, pericardium, pulmonary parenchyma, pleura, trachea and its bifurcation and major bronchus, ribs, abdominal organs, abdominal vessels and visceral situs.

Studies Interpretation

All images were evaluated by a radiologist and a cardiologist independently. Image sets were systematically interpreted for supra-aortic arch branches, aorta—from the root to bifurcation—for evaluation of aortic position, coarctation or interruption and collateral branches. The main pulmonary artery and its branches were evaluated for their location, diameter and confluence of the two main branches.

Evaluation for collateral vessel branches varied with patient age. The reviewers were unaware of the results of other imaging techniques. All images included axial, multiplanar reformat (MPR), maximum intensity projection (MIP) and volume rendering techniques (VRT) and were interpreted in one session.

Pulmonary veins were evaluated for "partial anomalous pulmonary venous return" (PAPVR) or "total anomalous pulmonary venous return" (TAPVR), patent ductus arteriosus (PDA), cardiac apex and heart chambers, interatrial or interventricular septal defects, pericardium, location, size and number of IVC and SVC. The gold standard methods for the diagnosis of vascular lesion were echocardiography, angiography and surgery.

For the final diagnosis, the results were compared with echocardiography and angiography.

Case Examples

Aortic Arch Anomalies

Multislice CT is one of the best tools for evaluation of aortic arch anomalies. It includes double aortic arch as two separate arches with larger size of the right arch or two arches with complete ring and tracheal compression.

Aberrant right subclavian artery, the most common type of vascular anomaly, affects 0.5% of the population (Fig. 1). It arises from proximal portion of descending thoracic aorta and passes posterior to the esophagus and usually dose not cause any symptoms.

Right-sided aortic arch passes to the right of the trachea and may descend either to the right or left of the thoracic spine (Fig. 2). Two types of aortic arch include right aortic arch with mirror image brachiocephalic branching and right aortic arch with aberrant left subclavian artery. Cervical aortic arch is a rare anomaly in which the aortic arch extends into the soft tissue of the neck. It may produce stridor or dyspnea.

Aortic Coarctation

Coarctation is a common congenital anomaly in which a stenotic segment causes obstructive stenosis. The stenotic segment can be focal aortic coarctation (Fig. 3), diffuse hypoplastic aortic arch, or complete aortic arch interruption (Fig. 4).

Aortic Pseudocoarctation

Pseudocoarctation is a rare anomaly and occurs when the third and seventh segments of the arch fail to fuse with resultant elongation of the arch and also the first portion of the descending aorta.

Fig. 1. Three-year old girl in whom the aortic arch could not be visualized by echocardiography. MDCT was requested to determine the anatomy of the aortic arch consist of anomalous arch branches as right subclavian, right common carotid, left common carotid and aberrant right subclavian artery volume rending technique (VRT) from posterior view.

Fig. 2. Four months old boy that aortic arch was not visualized with echocardiography. MDCT was requested to determine anatomy of aortic arch consist of right sided aortic arch and anomalous arch branches. VRT from anterior view.

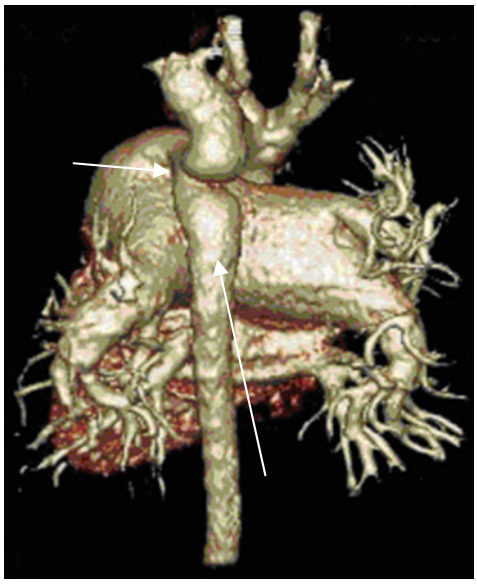

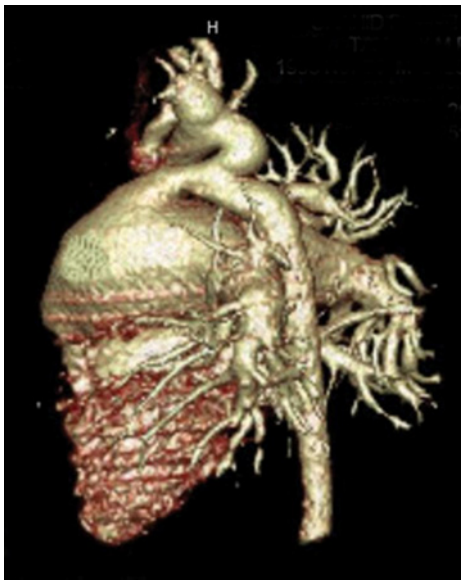

Fig. 3. Ten-year-old boy with severe aortic coarctation (large arrow) was referred for MDCT to evaluate other associated anomalies.

A and B. VRT images show ductus arteriosus (small arrow) as a connection between the descending thoracic aorta and pulmonary artery. The main pulmonary artery and its major branches reveal remarkable enlargement as a result of sever pulmonary hypertension (VRT from lateral and posterior view).

Intracardiac Shunts

Ventricular Septal Defect (VSD)

VSDs are classified according to the affected part of the ventricular septum. Membranous VSD is a small area just inferior to the root of the aorta between the right coronary cusp and the non-coronary cusp. Supracristal VSD just located below the pulmonary valve and the aortic valve is often called subaortic VSD. Muscular VSD is located in thick muscular part of the septum and can be multiple (Fig. 5).

Atrial Septal Defect (ASD)

The atrial septum is derived from several septa and ostia that form and involute which finally divides two atriums and includes ostium primum, ostium secundum and sinus venous type (Fig. 6).

Patent Ductus Arteriosus (PDA)

The connection that courses from the proximal descending aorta to the left pulmonary artery just beyond the pulmonary artery bifurcation (Fig. 7).

Aortopulmonary Window

There is a defect between the ascending aorta and main pulmonary artery with left to right shunt (Fig. 8).

Tetralogy of Fallot (TOF)

This anomaly consists of pulmonary stenosis, overriding of aorta, VSD, and right ventricular hyper-

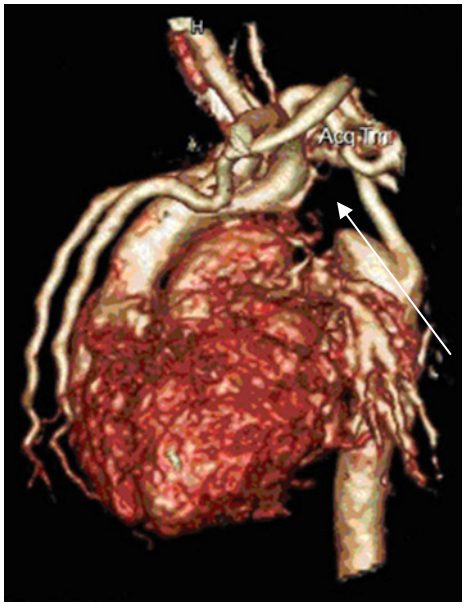

Fig. 4. Four-day-old boy with aortic interruption (arrow) and large intercostal collateral and enlarged internal mammary arteries.

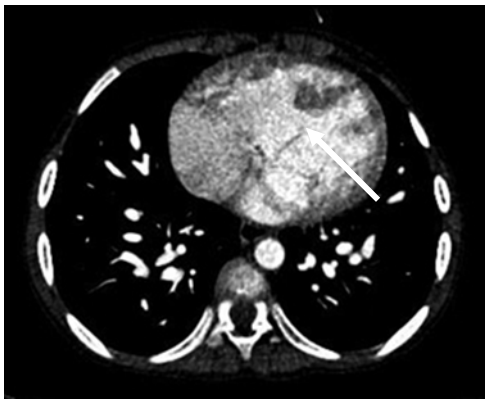

Fig. 5. Ten-year-old boy with Down syndrome presented with cyanosis and fainting. Axial images show large ventricular septal defect (arrow).

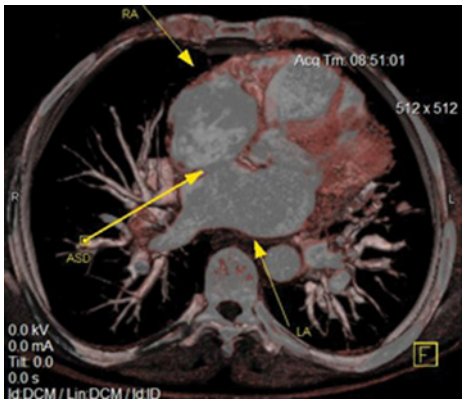

Fig. 6. Seventy two years old man with cyanosis and convulsion and high heart rate reveals large left to right shunt related to atrial septal defect (ASD).

Fig. 7. Five-month-old boy with patent ductus arteriosus (large arrow), aortic interruption (small arrow), and anomalous arch branches.

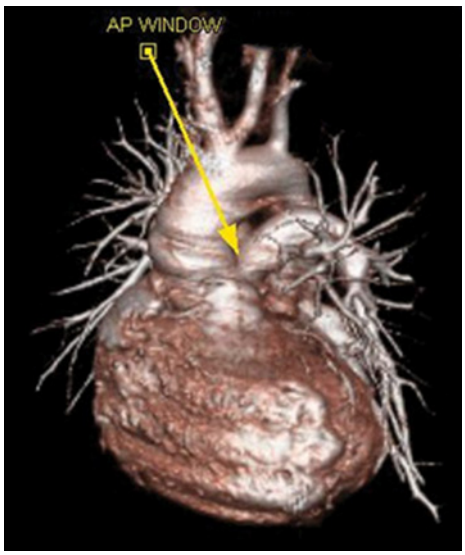

Fig. 8. Seventeen-year-old girl with left to right shunt and aortopulmonary window (arrow) as an opening between the ascending aorta and main pulmonary.

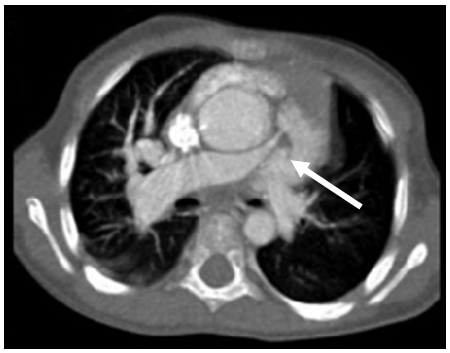

Fig. 9. Three-year-old girl with severe pulmonary stenosis (arrow) as a component of Tetralogy of Fallot (TOF).

Fig. 10. Hypoplastic right ventricle in a patient with TOF. Axial CT image shows a small right ventricle in contrast with the left ventricle.

trophy. The key feature of TOF is malalignment of the infundibular septum causing the right ventricular outflow to be small and the aorta to override the VSD (Figs. 9 and 10).

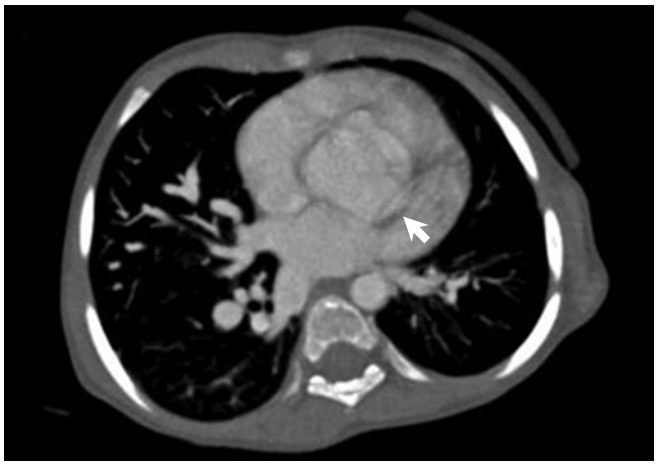

Fig. 11. Truncus arteriosus (arrow) in axial CT image reveals a single trunk above the ventricles without any pulmonary artery trunk

Fig. 12. Eight-year-old girl with cyanosis and convulsion shows type 1 truncus arteriosus. VRT image from anterior view. Aorta (arrow) and pulmonary artery (arrowhead).

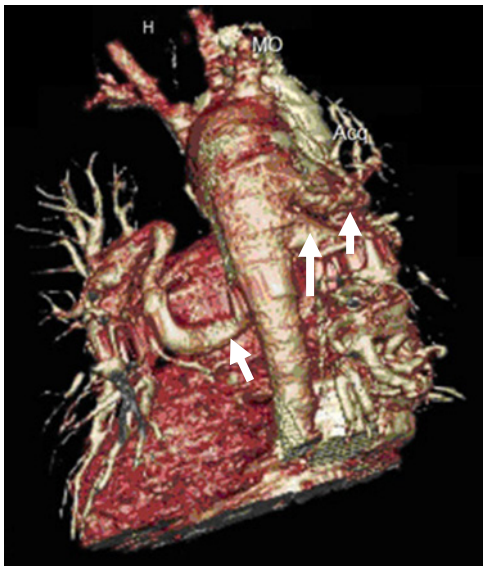

Fig. 13. Thirty-four-year old women with truncus arteriosus type 4 and multiple aortopulmonary collaterals (MAPCA) (arrows) as multiple large collaterals from descending thoracic aorta .VRT image from posterior view.

Truncus Arteriosus

In this anomaly, single arterial trunk form over both ventricles and the aorta and pulmonary arteries do not developed normally. It divides into four types.

In type 1, septum divides the origin of the aorta and pulmonary trunk. In type 2 the right and left pulmonary arteries are close to each other but arise from the trunk separately from posterior aspect of the trunk. In type 3, the right and left pulmonary arteries arise from lateral aspect of the trunk. In type 4, no pulmonary artery arises from the aorta but branches from the descending thoracic aorta supply pulmonary vasculature as multiple aortopulmonary collaterals (MAPCA). All types of truncus arteriosus are always associated with VSD (Figs. 11–13).

Transposition of Great Arteries (TGA)

In this anomaly, the major great arteries are displaced, aorta arises from the right ventricle, and pulmonary artery arises from the left ventricle (Figs. 14 and 15).

Systemic Venous Connections (SVC)

The most common anomalous systemic venous connection is the "persistent left-sided SVC," a remnant of the embryonic left anterior cardinal vein.

Interruption of IVC with azygos continuation is another anomaly of systemic veins (Fig. 16).

Total Anomalous Pulmonary Venous Connection (TAPVC)

Anomalous connection of pulmonary veins to sys-

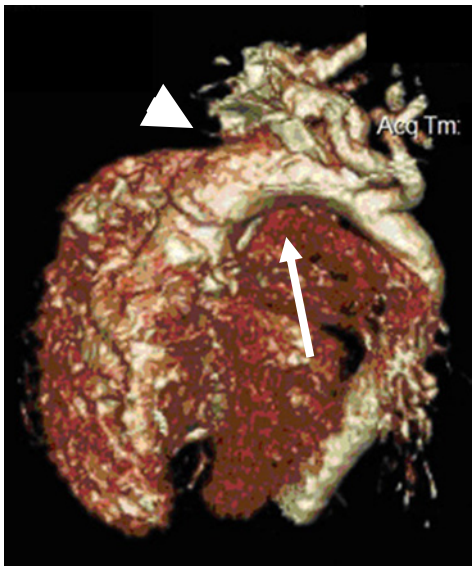

Fig. 14. Transposition of great arteries in volumetric images reveal anterior located aorta (arrow head) with connection to right ventricle and posterior location of pulmonary artery (arrow) from the left ventricle. VRT from lateral view.

Fig. 15. Six-year-old boy presented with apneic spell. Axial CT images reveal transposition of great arteries with anterior location of aorta (small arrow) and posterior location of pulmonary artery (large arrow) and its major branches.

temic vein instead of left atrium is called anomalous pulmonary venous connection (Figs. 17-19).

Partial Anomalous Pulmonary Venous Connection (PAPVC)

It can be diagnosed when one, two, or three pulmonary veins drain anomalously into the systemic circulation. In PAPVC the anomalous veins can drain into supracardiac (SVC, left vertical vein), cardiac (right atrium), or infracardiac (IVC) sites (Fig. 20).

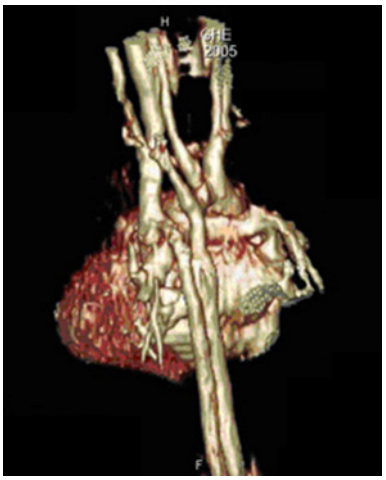

Fig. 16. Two-month-old girl was referred for poor feeding and multiple cardiac anomalies and azygos continuation of IVC (arrow).

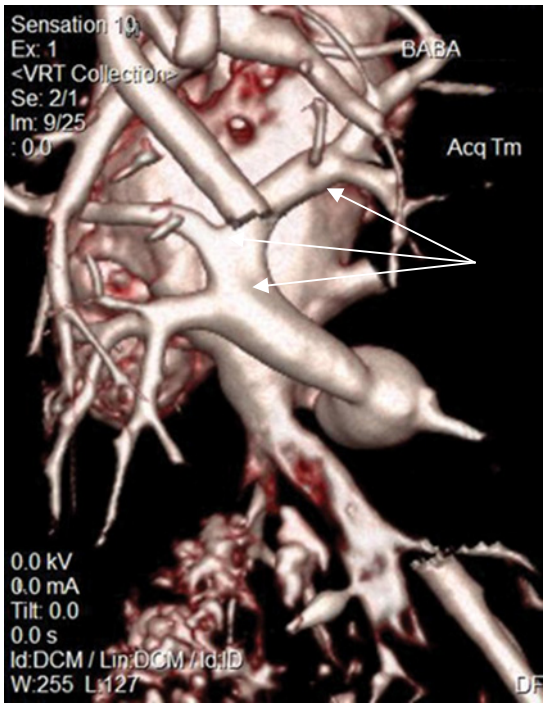

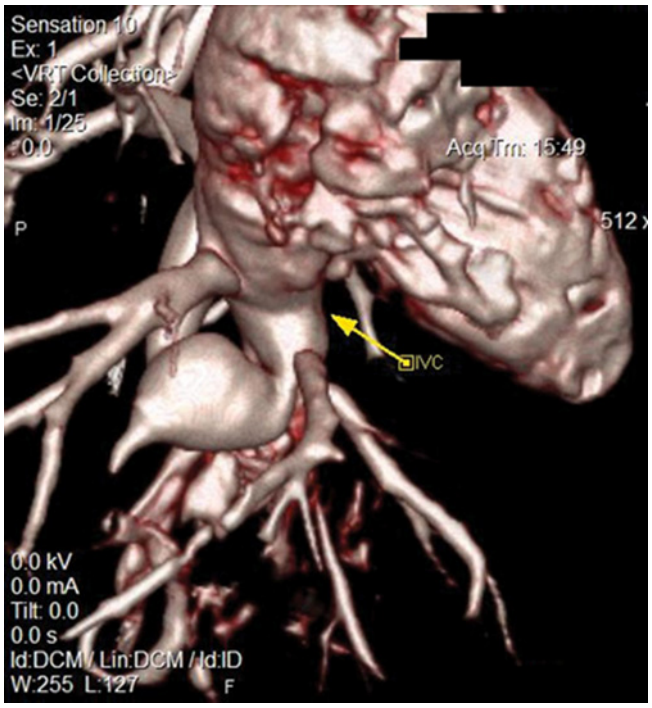

Fig. 17. A and B. Twelve-day-old boy presented with cyanosis, respiratory distress and hepatomegaly with total anomalous pulmonary venous return to infradiaphragmatic part of the inferior vena cava .VRT images from posterior (left) and anterior (right) views.

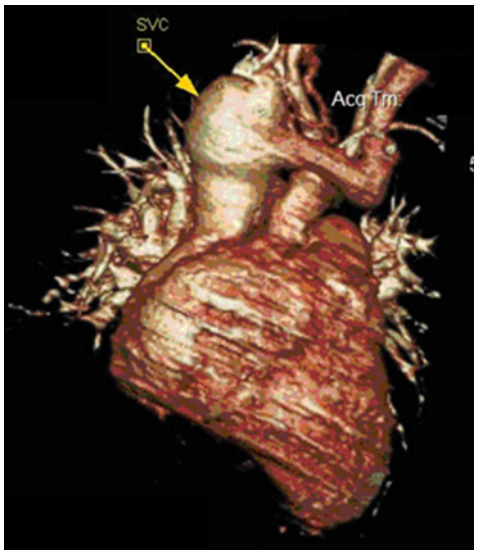

Fig. 18. Five-month-old boy with cyanosis, dyspnea and remarkable enlargement of SVC due to total anomalous pulmonary venous connection (TAPVC).

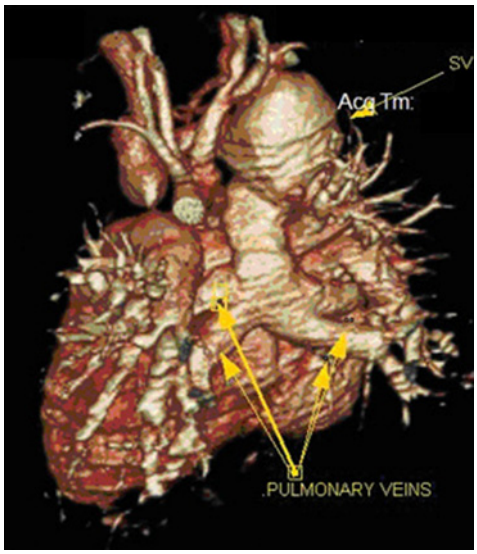

Fig. 19. Five-month-old boy with cyanosis, dyspnea, supracardiac total anomalous, with pulmonary venous connection (TAPVC) to SVC.

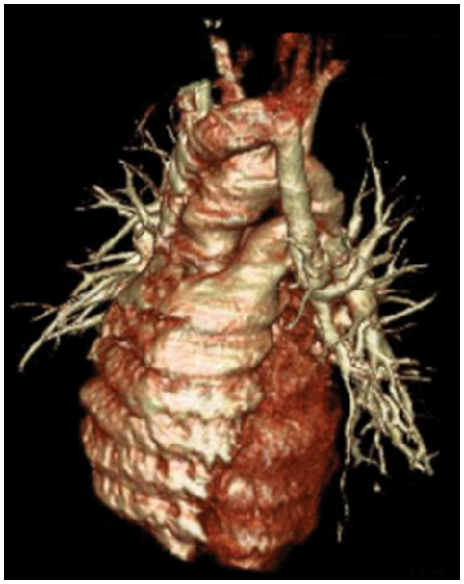

Fig. 20. Partial anomalous pulmonary venous return (PAPVR) (arrow) of left pulmonary veins to brachiocephalic venous system in a 23-year-old man with fatigue and dyspnea.

Fig. 21. Axial slice during dynamic contrast medium injection in a 13-year-old girl with single atrium and common atrioventricular canal.

Common Atrioventricular Canal

This anomaly results from abnormalities of the endocardial cushions that grow together in the center of the heart and divide the atria from the ventricles (Fig. 21).

Conclusion

This article presents use of MDCT in many situations of difficult congenital cardiac lesion seen in clinical practice. Multidetector technology provides important information with high accuracy and specifity for anatomic details of congenital heart disease for the referring cardiologist. One of the most important benefits of these modalities is the possibility of anatomic evaluation of different anatomic structures (*i.e.*, heart, great vessels, lungs and abdomen) in one acquisition. These technologic advances have produced diagnostic images with increased speed, multiple reconstructed images such as multiplanar reformat (MPR), maximum intensity projection (MIP) and volume rendering technique (VRT) with ability of review images by radiologist and workers repeatedly and markedly decreased the sedation time, and ease of peripheral venous access without angiography complications.

References

1. Gross GW, Steiner RM. Radiogrphic manifestation of congenital heart disease. Radiol Clin North Am 1991;29:293-317.
2. Haselgrove JC, Simonetti O. MRI for physiology and function: technical advances in MRI of congenital heart disease. Semin Roentgenol 1998;33:293-301.

3. Kaemmerer H, Stem H, Fratz S, Prokop M, Schwaiger M, Hess1 J. Imaging in adults with congenital cardiac disease (ACCD). Thoracic Cardiovascular Surg 2000;48:328-35.
4. Choi BW, Park YH, Choi JY, Choi BI, Kim MJ, Ryu SJ, et al. Using EBCT to evaluate conotruncal abnormalities in pediatric and adult patients. AJR 2001;177:1045-9.
5. Ravenel JG, Mc Adams HP, Remy J. Multidimensional imaging of the thorax: practical application. J Thoracic imaging 2001;16:269-81.